J Physiol 591.6 (2013) pp 1433–1445

The Journal of Physiology

STIM2 drives Ca^{2+} oscillations through store-operated Ca^{2+} entry caused by mild store depletion

Markus Thiel[1,2], Annette Lis[1,3] and Reinhold Penner[1]

[1] *Center for Biomedical Research, The Queen's Medical Center and University of Hawaii, Honolulu, HI 96813, USA*
[2] *Department of Internal Medicine I, Saarland University, D-66421 Homburg, Germany*
[3] *Institute of Biophysics, Saarland University, D-66421 Homburg, Germany*

Key points

- Stromal cell-interaction molecule (STIM) 2 senses Ca^{2+} levels in the endoplasmic reticulum and activates Ca^{2+} channels in the plasma membrane upon store depletion.
- Here we report that STIM2 is preferentially activated by low agonist concentrations that cause mild reductions in endoplasmic reticulum Ca^{2+} levels.
- This shows that store-operated Ca^{2+} entry is regulated through signal strength, with weak stimuli activating STIM2 and strong stimuli engaging STIM1.
- The results help us to understand how receptor activation enables differential modulation of Ca^{2+} entry over a range of agonist concentrations and levels of store depletion.

Abstract Agonist-induced Ca^{2+} oscillations in many cell types are triggered by Ca^{2+} release from intracellular stores and driven by store-operated Ca^{2+} entry. Stromal cell-interaction molecule (STIM) 1 and STIM2 serve as endoplasmic reticulum Ca^{2+} sensors that, upon store depletion, activate Ca^{2+} release-activated Ca^{2+} channels (Orai1–3, CRACM1–3) in the plasma membrane. However, their relative roles in agonist-mediated Ca^{2+} oscillations remain ambiguous. Here we report that while both STIM1 and STIM2 contribute to store-refilling during Ca^{2+} oscillations in mast cells (RBL), T cells (Jurkat) and human embryonic kidney (HEK293) cells, they do so dependent on the level of store depletion. Molecular silencing of STIM2 by siRNA or inhibition by G418 suppresses store-operated Ca^{2+} entry and agonist-mediated Ca^{2+} oscillations at low levels of store depletion, without interfering with STIM1-mediated signals induced by full store depletion. Thus, STIM2 is preferentially activated by low-level physiological agonist concentrations that cause mild reductions in endoplasmic reticulum Ca^{2+} levels. We conclude that with increasing agonist concentrations, store-operated Ca^{2+} entry is mediated initially by endogenous STIM2 and incrementally by STIM1, enabling differential modulation of Ca^{2+} entry over a range of agonist concentrations and levels of store depletion.

(Received 24 September 2012; accepted after revision 24 January 2013; first published online 28 January 2013)
Corresponding author R. Penner: Center for Biomedical Research, The Queen's Medical Center, 1301 Punchbowl St., Honolulu, HI 96813, USA. Email: rpenner@hawaii.edu

Abbreviations $[Ca^{2+}]_i$, intracellular free Ca^{2+}; CRAC, Ca^{2+} release-activated Ca^{2+} channel; ER, endoplasmic reticulum; LTC_4, leukotriene C_4; MeCh, metacholine; PBL, peripheral blood lymphocytes; PLCγ, phospholipase Cγ; tBHQ, tert-butylhydroquinone; TG, thapsigargin; SERCA, sarco/endoplasmic reticulum Ca^{2+}-ATPase; SOCE, store-operated Ca^{2+} entry; STIM, stromal cell-interaction molecule.

DOI: 10.1113/jphysiol.2012.245399

Introduction

Changes in intracellular free Ca^{2+} ($[Ca^{2+}]_i$) through Ca^{2+} release and/or Ca^{2+} entry regulate numerous cellular responses. Stimulated immunoreceptors such as Fc receptors in mast cells and T-cell receptors (TCR) in lymphocytes lead to the activation of phospholipase (PLC) γ and the production of inositol trisphosphate (IP_3), which releases Ca^{2+} from endoplasmic reticulum (ER) Ca^{2+} stores. The depleted Ca^{2+} stores then induce the opening of Ca^{2+} release-activated Ca^{2+} (CRAC) channels that permit sustained, store-operated Ca^{2+} entry (SOCE) into the cell (Parekh & Putney, 2005; Peinelt *et al.* 2006; Lewis, 2007; Putney, 2007). Recent work has identified the main molecular players of SOCE connecting Ca^{2+} release from stores to the opening of CRAC channels: the ER Ca^{2+} sensors stromal cell-interaction molecule (STIM) 1, STIM2 and the *Drosophila* homologue *D*-STIM (Williams *et al.* 2001; Stathopulos *et al.* 2006; Dziadek & Johnstone, 2007) as well as the CRAC channels *Drosophila* protein *D*-Orai (or -CRACM) and its three mammalian homologues, Orai1, Orai2 and Orai3 (or CRACM1, CRACM2 and CRACM3) (Feske *et al.* 2006; Prakriya *et al.* 2006; Vig *et al.* 2006*b*; Yeromin *et al.* 2006; Lis *et al.* 2007; Gwack *et al.* 2007). When STIM1 or STIM2 are overexpressed jointly with Orai proteins, they reconstitute large CRAC currents (Mercer *et al.* 2006; Lis *et al.* 2007; Parvez *et al.* 2008) and mutational analysis of Orai1 has revealed several key amino acids that determine the selectivity of CRAC currents (Prakriya *et al.* 2006; Vig *et al.* 2006*a*; Yeromin *et al.* 2006).

D-STIM, STIM1 and STIM2 are single pass transmembrane proteins in the ER membrane with paired amino-terminal EF-hands located in the luminal side of the ER (Williams *et al.* 2001; Roos *et al.* 2005; Dziadek & Johnstone, 2007; Yuan *et al.* 2009). Upon store depletion, STIM proteins translocate into junctional structures (puncta) close to the plasma membrane (Stathopulos *et al.* 2006; Wu *et al.* 2006; Xu *et al.* 2006; Smyth *et al.* 2008), where they may bind to and activate CRAC channels (Zhang *et al.* 2005; Luik *et al.* 2006; Wu *et al.* 2007; Lioudyno *et al.* 2008). The luminal STIM2 EF-hand has a lower Ca^{2+} affinity compared to STIM1 (Zheng *et al.* 2008), which may account for their different biological functions. In heterologous expression systems, SOCE elicited by receptor agonists and mediated by STIM2 is faster than that mediated by STIM1 (Parvez *et al.* 2008) and STIM2 translocates earlier to puncta after EGTA application compared to STIM1 (Brandman *et al.* 2007; Bird *et al.* 2009). Even in the endogenous system, STIM2 translocates earlier to puncta after metacholine (MeCh) application compared to STIM1 (Bird *et al.* 2009). While STIM1 operates exclusively in a store-operated manner, STIM2 exhibits both store-dependent and store-independent modes of CRAC channel activation (Liou *et al.* 2007; Parvez *et al.* 2008). Moreover, STIM2 can be modulated by calmodulin and is inhibited by the aminoglycoside antibiotic G418 (Parvez *et al.* 2008).

Most cells express both STIM1 and STIM2 (Williams *et al.* 2001) and both proteins are required for sustained NFAT signalling and cytokine production in T and B cells (Oh-Hora *et al.* 2008; Matsumoto *et al.* 2011). Whereas the functional role of STIM1 has been established as a Ca^{2+} sensor essential for SOCE, the situation is not as clear for its homologue STIM2. Heterologously expressed STIM2 appears to be constitutively active at rest (Brandman *et al.* 2007; Parvez *et al.* 2008) and although it can induce SOCE upon store depletion (Brandman *et al.* 2007; Oh-Hora *et al.* 2008; Parvez *et al.* 2008), its knockout does not suppress SOCE significantly when depleting stores via TCR or thapsigargin (TG) (Oh-Hora *et al.* 2008).

Investigation of the relative roles of STIM1 and STIM2 in SOCE is challenging for a number of reasons. First, STIM molecules aggregate and co-assemble into clusters upon store depletion (Darbellay *et al.* 2010). Thus, during moderate Ca^{2+} depletion the initial response might be mediated by STIM2 due to its lower Ca^{2+} affinity (Brandman *et al.* 2007; Zheng *et al.* 2008); however, this can also lead to co-clustering of STIM1 molecules, and ultimately both STIM molecules may contribute to activating CRAC channels even if the initial sensing were mediated exclusively through STIM2. A second complication arises from the constitutive activity of STIM2 itself (Brandman *et al.* 2007; Parvez *et al.* 2008), which endows this molecule to regulate both basal levels of Ca^{2+} in the cytosol and in the ER. This complicates the assessment of STIM2 function following molecular silencing through siRNA approaches, as the long-term downregulation of STIM2 activity will reduce ER Ca^{2+} levels, so that the relative threshold for the remaining STIM1 molecules is lowered. Bearing these factors in mind, we have investigated the physiological function of endogenous STIM proteins in *Drosophila* Kc cells, rat mast cells (RBL-1 and RBL-2H3), human embryonic kidney cells (HEK) and primary human lymphocytes with molecular, functional and pharmacological approaches. We find that at low levels of agonist stimulation endogenous STIM2 acts as the primary sensor that mediates SOCE and sustains agonist-mediated Ca^{2+} oscillations, whereas STIM1 becomes the dominant mechanism for driving SOCE under high agonist concentrations and strong store depletion.

Methods

Cell culture

RBL-1, RBL-2H3 and all HEK293 cells were cultured in DMEM (Life Technologies, Grand Island, NY, USA)

supplemented with 10% fetal bovine serum (FBS) and 1% glutamine. *Drosophila* Kc cells were cultured in Schneider's medium (Gibco, GE Healthcare, Piscataway, NJ, USA) supplemented with 10% FBS and 1% glutamine at 25°C. Peripheral blood lymphocytes (PBL) were cultured in RPMI 1640 (Life Technologies) supplemented with 10% FBS and 1% glutamine. PBL used for the Ca^{2+} imaging experiments were collected from healthy donors and purified as previously described (Renner *et al.* 1995). PBLs were isolated by density gradient centrifugation at 450 ***g*** for 30 min at RT (Ficoll-Paque™ plus, Amersham Biosciences, GE Healthcare, Picataway, NJ, USA) in 50 ml Leucosep tubes (Greiner, Solingen, Germany). The PBL layer was washed in PBS. The remaining red blood cells were removed by addition of 1 ml lysis buffer (155 mM NH_4Cl, 10 mM $KHCO_3$, 0.1 mM EDTA, pH 7.3) for 1 min. After lysis, cells were washed with PBS (200 ***g***, 10 min, RT) and kept in media for 1–3 days before use.

Subcloning and overexpression

Full length human CRACM1 was subcloned as described earlier (Lis *et al.* 2007). For electrophysiological analysis, CRACM1 protein was overexpressed in HEK293 cells stably expressing STIM2 protein (Soboloff *et al.* 2006) using Lipofectamine 2000 (Invitrogen, Carlsbad, CA, USA) and the GFP expressing cells were selected by fluorescence. Experiments were performed 24–72 h after transfection. HEK293 cells stably expressing STIM2 were grown for several weeks in the absence of G418 (500 μg ml^{-1}).

Electrophysiology

Patch clamp experiments were performed in the tight seal whole cell configuration at 21–25°C. Voltage ramps of 50 ms duration spanning a range of –100 to +100 mV were delivered from a holding potential of 0 mV at a rate of 0.5 Hz. All voltages were corrected for a liquid junction potential of 10 mV. Currents were filtered at 2.9 kHz and digitized at 100 μs intervals. Capacitive currents were determined and corrected before each ramp. Where applicable, statistical errors of averaged data are given as means ± S.E.M. with *n* determinations. Standard external solutions were as follows (in mM): 120 NaCl, 2.8 KCl, 2 $MgCl_2$, 10 $CaCl_2$, 10 CsCl, 10 Hepes, 10 glucose, pH 7.2 with NaOH, 300 mosmol l^{-1}. Standard internal solutions were as follows (in mM): 120 caesium glutamate, 10 caesium BAPTA, 3 $MgCl_2$, 0 or 4 (150 nM $[Ca^{2+}]_i$) or 5.7 (300 nM $[Ca^{2+}]_i$) $CaCl_2$, 10 Hepes, pH 7.2 with CsOH, 300 mosmol l^{-1}. In some experiments, TG, or tert-butylhydroquinone was added to the standard external solution at a final concentration as indicated and applied using a wide mouth glass pipette. As indicated in the figure legends for some experiments, sodium orthovanadate (Na_3VO_4), G418, IP_3 or anti-STIM2 antibody (Anaspec, San Jose, CA, USA) were added to the internal solution. Anti-STIM2 antibodies were dialysed against PBS before use. $[Ca^{2+}]_i$ was buffered to defined levels using 10 mM caesium·BAPTA and appropriate concentrations of $CaCl_2$ as calculated with WebMaxC (http://www.stanford.edu/čpatton/webmaxcS.htm). All chemicals were purchased from Sigma (St. Louis, MO, USA).

Knockdown procedures

The CRACM1 knockdown in Kc cells was performed as described previously (Vig *et al.* 2006*b*). For the dsRNA knockdown of *D*-CRACM the Kc cells were diluted to a final concentration of 1×10^6 cells ml^{-1} in serum-free Schneider's medium. The resuspended cells were plated (1 ml per well) in six-well plates. Double-stranded RNA was added directly to the serum-free medium (15 μg) and the cells were incubated for 40 min at RT followed by addition of 3 ml of Schneider's medium containing FBS. The experiments were performed on day 3 of the knockdown.

For the transient knockdown of STIM proteins, RBL-2H3 and HEK293 cells were plated in a six-well plate and transfected with Stealth RNAi™ siRNA (Invitrogen) using Lipofectamine 2000 (Invitrogen) in combination with pCAGGSM2-IRES-GFP vector for green cell selection. Briefly, 25 pmol Stealth RNAi™ against STIM1 (HSS110308, HSS110309 and HSS110310), STIM2 (HSS126559, HSS126560 and HSS126561) and Stealth RNAi™ Negative control were transfected with 5 μl Lipofectamine and 1 μg pCAGGSM2-IRES-GFP using the standard cotransfecting protocol for mammalian cells. After 12 h incubation period the media was replaced and the cells transferred to coverslips. The experiments were performed on days 1, 2 and 3 post-transfection. The efficiency of the knockdown was determined by Western blot analysis.

Preparation of cell extracts, immunoprecipitation and Western blotting

RBL-2H3 and HEK293 cells were harvested at the indicated time points after transfection, washed in PBS and lysed in 1 ml lysis buffer (in mM): 75 NaCl, 40 NaF, 10 Iodocetamide, 50 Hepes, 10% IGEPAL, 1 phenylmethylsulphonyl fluoride and protease inhibitor cocktail (Sigma). After incubation for 30 min by 4°C, the lysates were centrifuged and the supernatants retained. The cell lysates from RBL-2H3 (see Fig. 2) were precipitated with anti-STIM2(CT) rabbit polyclonal antibody (2.5 μg; Anaspec) for 1.5 h at 4°C and resolved

by SDS-PAGE. The protein concentrations from HEK293 cells lysates (see Supplementary Fig. S6) were determined using the Bradford assay. Protein samples (100 μg of total lysate) were resolved by SDS-PAGE and analysed using anti-STIM1 mouse antibody (BD Bioscience, San Diego, CA, USA), anti-STIM2(CT) rabbit polyclonal antibody (Anaspec) or anti-GAPDH mouse monoclonal (Abcam, Cambridge, MA, USA) at a dilution 1:500, 1:600 and 1:5000. Antirabbit IgG or antimouse IgG (whole molecule) peroxidase conjugate (Sigma) was used as a secondary antibody according to the manufacturer's instructions. Proteins were detected by developing with ECL Plus Western Blotting Detection System (Amersham) or with SuperSignal West Femto Maximum Sensitivity Substrate (Thermo Scientific, Rockford, IL, USA).

Calcium measurements

For Ca^{2+} measurements, cells were loaded with 2 μM Fura-2 AM (Molecular Probes, Eugene, OR, USA) for 60 min in media at 37°C. For Ca^{2+} oscillation measurements in RBL-1 cells and HEK293 cells, cells were loaded with 2 μM Fura-FF AM (Molecular Probes) for 45 min in media at 37°C. In some experiments, 500 μg ml^{-1} G418 was added to the Fura-2 AM or Fura-FF AM containing medium and maintained in the bath solution for Ca^{2+} measurements. After Fura loading, cells were washed and kept in extracellular saline containing (in mM): 140 NaCl, 2.8 KCl, 2 $MgCl_2$, 0 or 1 $CaCl_2$, 11 glucose, 10 Hepes-NaOH, pH 7.2. For Ca^{2+} oscillation measurements in RBL-1 cells and HEK293 cells, extracellular saline was modified (in mM): 120 NaCl, 5.4 KCl, 0.8 $MgCl_2$, 0 or 1.8 $CaCl_2$, 11 glucose, 20 Hepes-NaOH, pH 7.3. After cells were loaded with Fura, they were kept in external Ringer's as described for electrophysiological experiments and Ca^{2+} entry was induced by application of adequate stimuli in external Ringer's solution. PBL were stimulated with antihuman CD3 (BD Pharmingen, clone UCHT1, San Diego, CA, USA), RBL-1 with leukotriene C_4 (LTC_4), RBL-2H3 cells with TG and HEK293 cells with MeCh. IgE-dependent activation was achieved for cells preincubated with 0.5 μg ml^{-1} anti-DNP (Sigma) for 16 h with subsequent application of DNP-BSA (Sigma). Experiments were performed at RT with a Zeiss Axiovert 100 fluorescence microscope equipped with a dual excitation fluorometric imaging system (TILL-Photonics, Gräfelfingen, Germany), using a 40× Plan NeoFluar objective. Data acquisition and computation was controlled by TILLvisION software. Dye-loaded cells were excited by wavelengths of 340 and 380 nm delivered by a monochromator (Polychrome IV). The fluorescence emission was simultaneously recorded with a video camera (TILL-Photonics Imago) using an optical 440 nm longpass filter. The signals were sampled at 0.5 or 0.17 Hz and computed into background-corrected relative ratio units of the fluorescence intensity at different wavelengths (F_{340}/F_{380}). Typically, 30–50 regions of interest were monitored per experiment. All measurements represent a minimum of three independent experiments.

Statistics

Where applicable, statistical errors of averaged data are given as means ± S.E.M. with n determinations and statistical significance assessed by Student's t test.

Results

Sarcoplasmic reticulum/ER Ca^{2+}-ATPase (SERCA) inhibitors have been extensively used to study effects of passive ER Ca^{2+} store depletion on SOCE and CRAC channel activation (Thastrup *et al.* 1990; Broad *et al.* 1999). Passive depletion protocols rely on leak pathways and therefore show delayed activation of SOCE compared to active protocols such as IP_3 (Hoth & Penner, 1992), providing a means to reduce ER Ca^{2+} levels slowly and gradually. We perfused RBL-2H3 cells with different internal concentrations of orthovanadate, a known SERCA inhibitor (Dormer *et al.* 1993), and assessed its efficacy in activating I_{CRAC}. At high concentrations of 50 μM to 5 mM vanadate, the magnitude and kinetics of I_{CRAC} were similar (Fig. 1*A*), but still exhibited a marked delay in activation of 30–60 s that was significantly longer than the 2–6 s delays typically observed with 20 μM IP_3. This observation differs from a previous report (Ehring *et al.* 2000), where vanadate activated CRAC channels with kinetics comparable to IP_3. At lower concentrations of vanadate (5 μM), we observed even longer delays of ∼110 s in the onset of the current (Fig. 1*A*), although the final amplitudes were similar regardless of concentration. In all cases, vanadate-induced currents exhibited the typical inwardly rectifying current–voltage (I–V) relationship of I_{CRAC} (Fig. 1*B*). These data suggest that vanadate dose-dependently inhibits SERCA, which leads to gradual store depletion and ultimately full activation of I_{CRAC}.

G418 is an aminoglycoside antibiotic that inhibits STIM2 without significantly affecting STIM1 (Parvez *et al.* 2008). Although aminoglycosides can have side effects, G418's specific activity against STIM2 makes it a valuable pharmacological tool in the context of SOCE. To distinguish between STIM1- and STIM2-mediated CRAC channel activation, we performed identical experiments in the presence of G418. Cells internally perfused with 10 μM G418 failed to activate I_{CRAC} when stimulated by 5 μM vanadate (Fig. 1*C*), indicating that at low levels of vanadate, the current was exclusively mediated by STIM2. Consistent with this idea, higher concentrations of vanadate of 50 μM produced normal I_{CRAC} activation

that remained unaffected by even 100 μM G418 (Fig. 1*D*), suggesting that complete store depletion was able to elicit CRAC channel activation independently of STIM2 and likely via STIM1. To further assess the specificity of this G418 effect and the involvement of STIM2, we perfused cells with a specific antibody recognizing the C-terminal cytosolic part of STIM2. Similar to G418, we observed a significant inhibition of the current induced by 5 μM vanadate (Fig. 1*E*). The slightly lower efficacy of the antibody compared to G418 may be due to its large molecular weight, which results in slower and less complete access to the cytosol through the patch pipette. A control antibody directed at the luminal N-terminus of STIM2 did not affect the current induced by 5 μM vanadate (Fig. 1*F*). In addition, we confirmed that the C-terminus antibody was ineffective in suppressing I_{CRAC} activated by high concentrations of vanadate (Fig. S1). Together, these data demonstrate that activation of CRAC channels by mild store depletion induced by low concentrations of vanadate is primarily mediated by STIM2.

If mild store depletion causes CRAC channel activation through STIM2, alternative ways of passive store depletion should have a similar effect. Buffering $[Ca^{2+}]_i$ to zero by cell dialysis with 20 mM BAPTA is equivalent to SERCA inhibition in that the buffer withholds Ca^{2+} from uptake into the ER (Hoth & Penner, 1992, 1993), resulting in gradual store depletion due to leakage of Ca^{2+} out of intracellular stores into the cytosol. As illustrated in Fig. S2*A*, G418 clearly delayed the current elicited under these conditions, although it did not abolish it. This delayed activation would be consistent with the notion that G418 suppressed the initial STIM2-mediated activation phase at moderate levels of store depletion; however, progressive lowering of store Ca^{2+} eventually reached the threshold for STIM1-mediated activation of I_{CRAC}, which is not susceptible to G418 inhibition.

In further experiments, we externally applied the prototypical SERCA inhibitor TG at 2 μM, with internal $[Ca^{2+}]_i$ buffered to 150 nM. As illustrated in Fig. S2*B*, TG elicited I_{CRAC} with some delay, consistent with passive store depletion. Again, intracellular perfusion of 10 μM G418 significantly reduced the TG-induced current, suggesting that under these experimental conditions of slightly elevated $[Ca^{2+}]_i$, TG-induced store depletion was mild and I_{CRAC} was triggered primarily by STIM2. The activation of a STIM1-mediated CRAC current may have been prevented by the slightly elevated $[Ca^{2+}]_i$ and TG-insensitive pumps, which have been demonstrated to

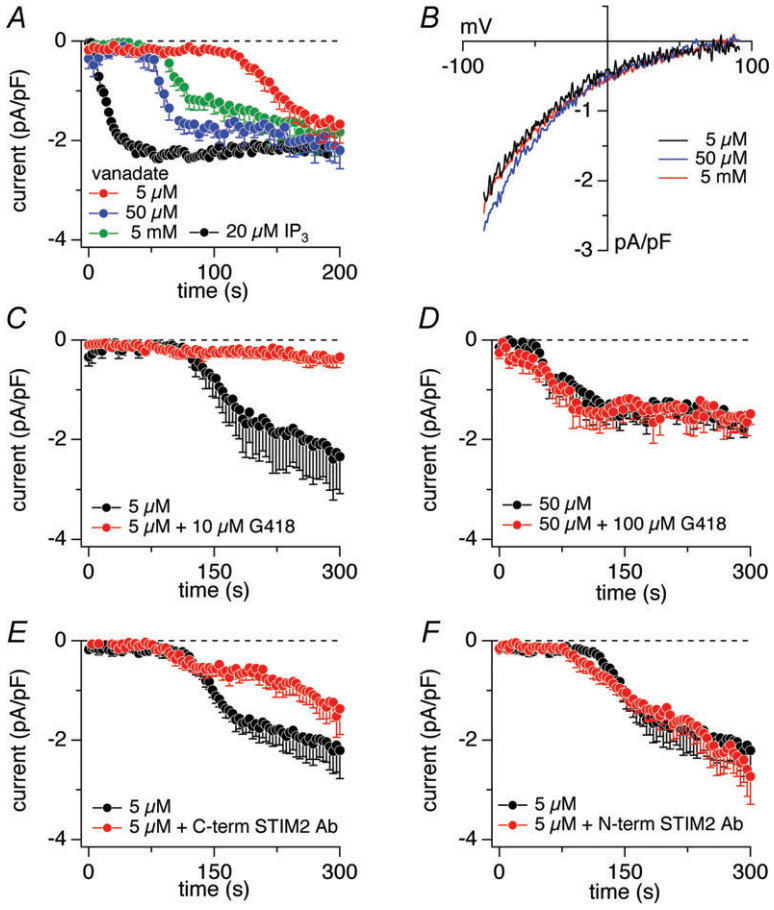

Figure 1. Vanadate effects in RBL-2H3 cells
$[Ca^{2+}]_i$ was clamped to 150 nM with 10 mM BAPTA and 4 mM $CaCl_2$. Data represent average leak-subtracted current densities (pA/pF ± S.E.M.) evoked by 50 ms voltage ramps from –100 to +100 mV extracted at –80 mV. *A*, average CRAC current densities with 5 μM ($n = 9$), 50 μM ($n = 8$), 5 mM ($n = 10$) vanadate or 20 μM IP_3 ($n = 5$). *B*, average *I–V* relationships of CRAC currents extracted from representative cells shown in (*A*) at 200 s. *C*, average CRAC current densities elicited by 5 μM vanadate in the absence ($n = 7$) and presence ($n = 9$) of 10 μM G418. *D*, same as *C* but using 50 μM vanadate in the absence ($n = 6$) or presence ($n = 9$) of 100 μM G418. *E*, average CRAC current densities elicited by 5 μM vanadate in the absence ($n = 10$) and presence ($n = 13$) of 10 μg ml^{-1} C-terminal STIM2. *F*, same as *E* but in the absence ($n = 10$) or presence ($n = 12$) of 10 μg ml^{-1} N-terminal STIM2 antibody. Ab, antibodies; CRAC, Ca^{2+} release-activated Ca^{2+}; IP_3, inositol trisphosphate; STIM, stromal cell-interaction molecule.

be present in RBL-2H3 cells (Turner *et al.* 2003). Another SERCA pump inhibitor (tert-butylhydroquinone was not very effective in activating I_{CRAC} in RBL-2H3; Fig. S2*C*).

The above experiments demonstrate that in RBL-2H3 cells, aside from intracellularly administered vanadate, the external application of the membrane-permeable SERCA inhibitor TG is an adequate and efficient external stimulus for SOCE. We therefore tested G418 for efficacy in interfering with SOCE in intact Fura-2-AM-loaded cells exposed to different concentrations of TG in the presence and absence of extracellular Ca^{2+} (Fig. S3). Here, store depletion mediated by TG elicited large increases in $[Ca^{2+}]_i$ over ∼8 min and then decayed to a lower steady state (Fig. S3*A*–*C*). G418 by itself had only a minor effect on cells exposed to control saline (Fig. S3*F*), but was effective in partially suppressing the Ca^{2+} response at all concentrations of TG, most strongly suppressing the response to the lowest concentration tested (20 nM; Fig. S3*C*). The G418-sensitive fractions (blue areas in Fig. S3*A*–*C*) were obtained by subtracting the Ca^{2+} responses in the absence of G418 from those obtained in its presence. We quantified the contribution of the G418-sensitive fraction to the total TG-induced Ca^{2+} response by calculating the percentage of the integral of the G418-sensitive fraction (Fig. S3*D*). At the two highest concentrations of TG, the contribution of the G418-sensitive component was 34% and 31% of the Ca^{2+} response and grew to 62% at the lowest TG concentration, confirming that STIM2 significantly contributes to SOCE in RBL-2H3 cells.

The main difference between these experiments and those performed by patch clamp relates to apparent potency differences of TG. In patch clamp recordings, we observed nearly complete suppression of 2 μM TG-induced I_{CRAC} by G418, whereas in intact cells the Ca^{2+} signal evoked by 2 μM was suppressed by 34%. As even small CRAC currents can lead to significant Ca^{2+} entry, the differences may not be as pronounced as they might appear. Even so, a slightly lower efficacy of TG in patch clamp experiments is to be expected, as its concentration in the cytosol is likely reduced during patch clamp experiments due to diffusional exchange with the pipette solution. Experiments performed in the absence of extracellular Ca^{2+} showed that Ca^{2+} signals evoked in Ca^{2+}-free medium were insensitive to G418 (Fig. S3*E*).

To further confirm our observations obtained from pharmacological intervention with G418 and antibodies against STIM2, we performed knockdown experiments in RBL-2H3 with siRNA specific for STIM2. On day 1 of the STIM2 knockdown, the response to 5 μM vandate was strongly suppressed (Fig. 2*A*), suggesting that STIM2 was indeed responsible for effective I_{CRAC} activation at low levels of store depletion. This effect was specific for STIM2, as these cells exhibited normal IP_3-mediated (Fig. 2*B*) and high vanadate-induced (500 μM) currents (Fig. 2*C*) compared to control cells, indicating uncompromised STIM1 signalling. Interestingly, however, after 48 h of siRNA treatment, the inhibitory effect of the knockdown in response to 5 μM vanadate was gone and I_{CRAC} developed normally (Fig. 2*D*). This was not caused by renewed expression of STIM2, as Western blot analysis revealed that the siRNA treatment suppressed STIM2 expression after 48 h even more effectively than after 24 h (Fig. 2*F*). Densitometric analysis yielded STIM2 expression levels of 36% on day 1 and 13% on day 2 relative to controls of that day. The low vanadate-induced current could not be suppressed by G418 (Fig. 2*E*), indicating that the current evoked by low vanadate concentrations on day 2 of the knockdown was now due to STIM1 rather than STIM2.

At first, this result may seem puzzling, however, it is consistent with a model, where STIM2 knockdown reduces basal $[Ca^{2+}]_i$ levels (Brandman *et al.* 2007) and thereby reduces ER Ca^{2+} levels to the extent that a further reduction of ER Ca^{2+} levels by low-level SERCA inhibition through vanadate now can reach the threshold for STIM1 activation. Thus, knockdown of STIM2 can be at least partially compensated for by functional sensitization of SOCE to STIM1, where the threshold for STIM1 activation is reduced by lowered ER Ca^{2+} concentrations. This notion is supported by experiments that assessed the basal ER Ca^{2+} content before and after loss of STIM2 for 24 h *vs.* 48 h (Fig. 2*G*–*I*). Here, we tested ER Ca^{2+} levels by quantifying Ca^{2+} release resulting from addition of the SERCA inhibitor TG in the absence of external Ca^{2+}, which reflects the releasable Ca^{2+} from ER Ca^{2+} stores that are functionally coupled to SOCE. Clearly, the knockdown of STIM2 progressively decreased TG-releasable Ca^{2+} in the stores. As a result, moderate Ca^{2+} release activity from already lowered Ca^{2+} levels in the stores might suffice to reach the threshold of STIM1-dependent SOCE.

As a complementary approach to the knockdown of STIM2 in RBL-2H3 cells, we also studied the *Drosophila* Kc cell line, which features a simplified SOCE system that accomplishes SOCE with one STIM sensor (*D*-STIM), one CRAC channel (*D*-CRACM or *D*-Orai) and one SERCA isoform. As in RBL-2H3 cells, vanadate was able to activate I_{CRAC} in Kc cells by virtue of inhibiting SERCA, resulting in dose-dependent I_{CRAC} activation (Fig. S4*A*). The *I*–*V* relationships of the resulting currents were very similar for all concentrations and exhibited typical inward rectification (Fig. S4*B*). Importantly, the current that was activated by the lowest effective vanadate concentration (30 μM) remained unaffected by the addition of 100 μM G418 in the patch pipette (Fig. S4*C*). These results are entirely consistent with the simplified molecular makeup of *Drosophila* cells, which rely on a single STIM molecule (*D*-STIM) to activate CRAC channels. The lack of effect of G418 further attests to the specificity of this aminoglycoside for STIM2 relative to other structurally

related STIMs such as STIM1 and *D*-STIM. Consistent with previous work (Vig *et al.* 2006*b*), the knockdown of *D*-CRACM not only completely eliminated store-operated currents induced by IP_3, but also those activated by 500 μM vanadate (Fig. S4*D*), further confirming that vanadate-induced currents were in fact carried by CRAC channels.

Although I_{CRAC} is the crucial Ca^{2+} influx mechanism driving IgE-dependent activation of RBL-2H3 cells (Hoth & Penner, 1992), little is known about the relative role of STIM2 in these cells. A recent study in RBL-1 cells found no role for STIM2 in shaping Ca^{2+} oscillations evoked by low concentrations of LTC4 through GPCR signalling, but did find STIM2 participated in SOCE activated through IgE receptors (Kar *et al.* 2012). To determine the role and participation of STIM2 in SOCE in native RBL-2H3 cells, we performed antigen-induced cross-linking of FcεRI and assessed the impact of the STIM2 inhibitor G418. Vehicle control measurements without agonist were performed with standard saline application and produced

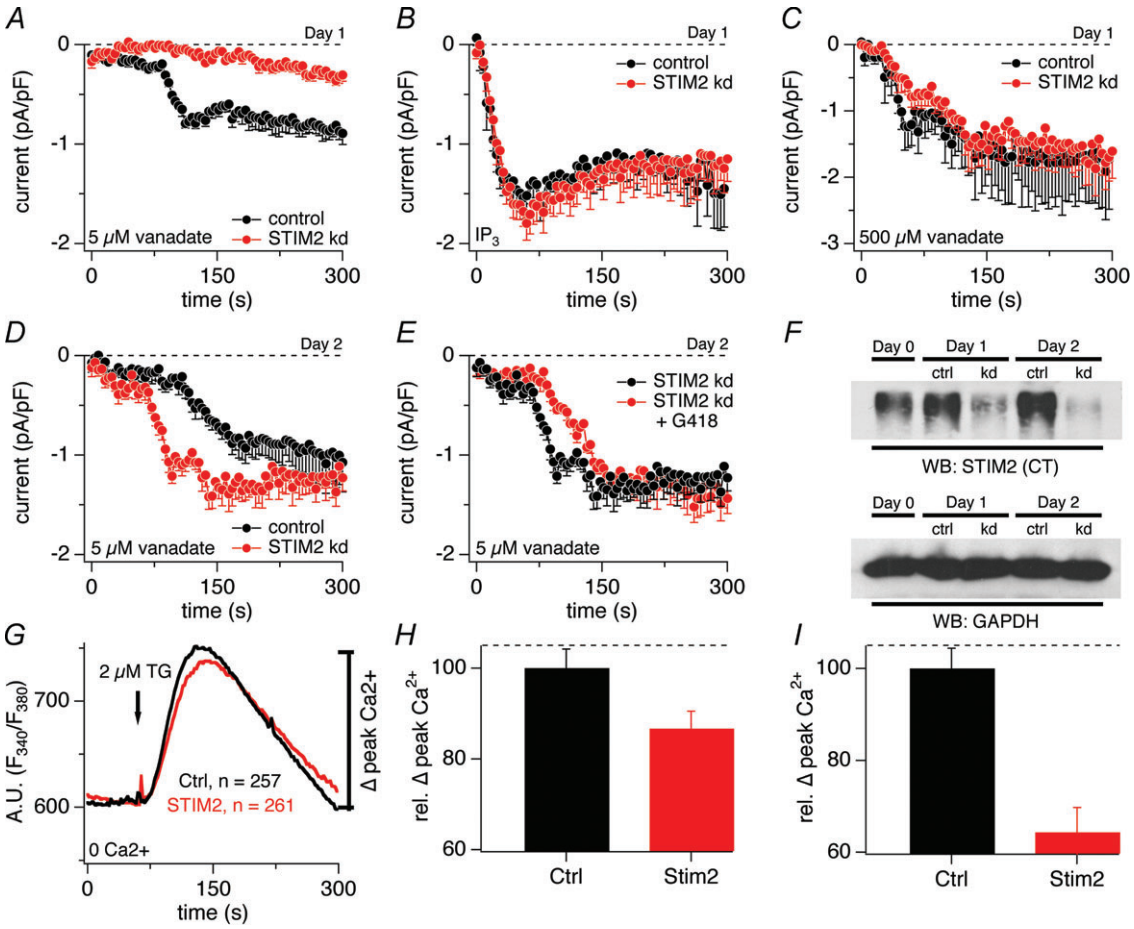

Figure 2. Effects of STIM2 knockdown on vanadate-induced I_{CRAC}
$[Ca^{2+}]_i$ was clamped to 150 nM. Data represent average leak-subtracted current densities (pA/pF ± S.E.M.) evoked by 50 ms voltage ramps from −100 to +100 mV extracted at −80 mV. Average CRAC current densities induced in RBL-2H3 by (*A*) 5 μM vanadate (control, $n = 13$; STIM2 kd cells, $n = 14$); (*B*) 20 μM IP_3 (control, $n = 6$; STIM2 kd, $n = 5$); and (*C*) 500 μM vanadate (control, $n = 6$; STIM2 kd, $n = 5$) on day 1 post-transfection. *D*, same as *A*, RBL-2H3 control ($n = 6$) and STIM2 kd cells ($n = 6$) induced by 5 μM vanadate on day 2 post-transfection. *E*, STIM2 kd cells stimulated with 5 μM vanadate in the absence ($n = 6$, same as in *D*) and presence ($n = 8$) of 10 μM G418. *F*, STIM2 siRNA specificity was assayed by immunoprecipitation and Western blot. RBL-2H3 cells were transfected with siRNA targeting STIM2 or control for 0, 1 and 2 days. Equal amounts of protein from total lysates were immunoprecipitated with anti-STIM2 C-terminal antibody. Immune complexes were resolved on SDS-PAGE gel and immunoblotted with anti-STIM2 C-terminal antibody. As control, equal amounts of total lysates from transfected RBL-2H3 cells were immunoblotted with anti-GAPDH antibody. *G*, endoplasmic reticulum Ca^{2+} levels were measured by the magnitude of Ca^{2+} release following addition of the SERCA inhibitor thapsigargin (2 μM) in Ca^{2+}-free solution on day 1 post-transfection. *H* and *I*, the relative ER Ca^{2+} levels based on Ca^{2+} transient amplitudes (Δpeak) on day 1 (*H*) and day 2 (*I*) in RBL-2H3 cells transfected with siRNA specific for STIM2. Ab, antibodies; CRAC, Ca^{2+} release-activated Ca^{2+}; IP_3, inositol trisphosphate; kd, knockdown; STIM, stromal cell-interaction molecule.

no significant changes in $[Ca^{2+}]_i$ regardless of whether cells had been pretreated with G418 or not (Fig. S5*C*). The typical, average response of sensitized RBL-2H3 cells to IgE-directed DNP-BSA stimulation (100 ng ml^{-1}) was a wave-like increase in $[Ca^{2+}]_i$ (Fig. 3*A*), with individual cells typically showing oscillatory spikes riding on top of a slow wave of elevated $[Ca^{2+}]_i$ (Fig. S5*A*). When cells were preincubated with G418, the same agonist concentration resulted in a smaller average $[Ca^{2+}]_i$ response (Fig. 3*A*) as well as smaller individual spikes (Fig. S5*B*). This indicates that the response was due to activation of both STIM1 and STIM2, with STIM2 contributing a small portion of receptor-mediated SOCE even at maximal stimulation of receptors.

We next asked whether a lower agonist concentration would change the relative contribution of STIM2 to the Ca^{2+} signals, as might be expected if it were preferentially activated by mild store depletion. Interestingly, decreasing the concentration of DNP-BSA to 10 ng ml^{-1} produced a more vigorous initial $[Ca^{2+}]_i$ signal that was more transient than the slow wave observed at 100 ng ml^{-1}, but was significantly more susceptible to G418 inhibition (Fig. 3*B*). The analysis of Ca^{2+} oscillations revealed that G418 preincubation reduced the average number of spikes at both stimulus intensities, but more strongly at lower agonist concentrations (Fig. 3*C* and *D*). Thus, the effect of G418 comprises both the reduction of Ca^{2+} oscillation frequency as well as reduced amplitudes

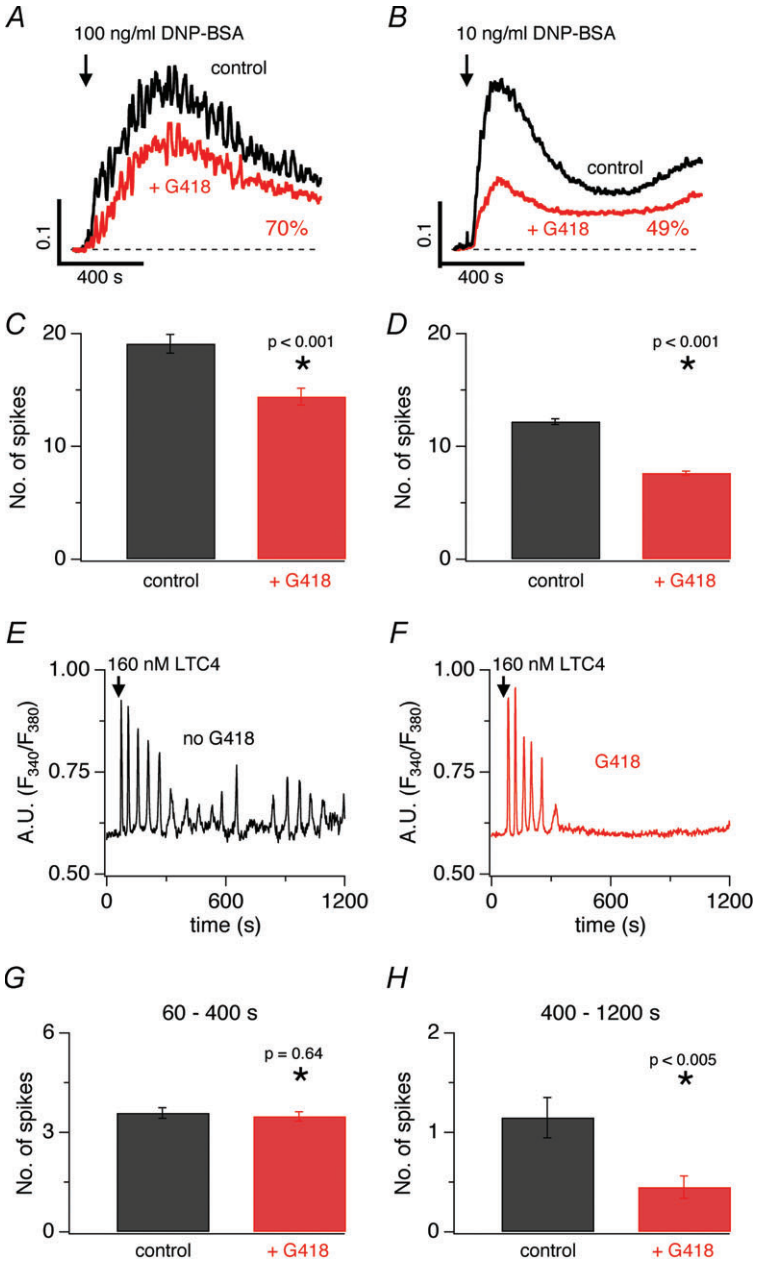

Figure 3. Inhibition of IgE-mediated Ca^{2+} signals by G418 in RBL-2H3 cells and LTC_4-mediated Ca^{2+} signals by G418 in RBL-1 cells
RBL-2H3 (*A–D*) and RBL-1 (*F–H*) were preincubated for 1 h in the absence or presence of G418 (500 μg ml^{-1}). The arrow indicates the application of DNP-BSA or LTC_4. Error bars indicate S.E.M. *A*, average intracellular Ca^{2+} changes (F_{340}/F_{380}) in RBL-2H3 cells elicited by 100 ng ml^{-1} DNP-BSA in control ($n = 110$) or preincubated cells ($n = 131$). *B*, same as *A* (10 ng ml^{-1}) DNP-BSA stimulation in control ($n = 784$) or preincubated cells ($n = 1139$). *C* and *D*, average number of spikes during 1200 s ($P < 0.001$) after 100 ng ml^{-1} (*C*) or 10 ng ml^{-1} (*D*) DNP-BSA stimulation in the same cells as shown in *A* and *B*. *E* and *F* intracellular Ca^{2+} changes (F_{340}/F_{380}) in a representative RBL-1 cell after stimulation with 160 nM LTC_4 in control (*E*) or preincubated with G418 (*F*). *G*, average number of spikes during the first 340 s ($P = 0.64$) and 400–1200 s ($P < 0.005$) into the experiment after LTC_4 stimulation (160 nM). kd, knockdown; LTC_4, leukotriene C_4; STIM, stromal cell-interaction molecule.

of individual spikes, indicating that both STIM1 and STIM2 contribute to Ca^{2+} oscillations at low and high agonist concentrations, with the relative contributions of both sensors shifting in favour of STIM2 at low agonist levels. These results are similar to those obtained by siRNA knockdown of STIM2 in RBL-1 cells (Kar *et al.* 2012).

RBL-1 cells can also generate Ca^{2+} oscillations through G protein-coupled receptors, e.g. cysteinyl leukotriene receptor 1 (CysLT1) via LTC_4, which generate IP_3 through stimulation of PLCβ, and these oscillations are primarily driven by pulsatile Ca^{2+} release from intracellular stores (Di Capite *et al.* 2009; Kar *et al.* 2012). Although these oscillations can be maintained for some time even in the absence of extracellular Ca^{2+}, sustained oscillatory activity at given frequencies also requires CRAC channel activity. A recent study found that siRNA knockdown of STIM2 had no effect on LTC_4-mediated Ca^{2+} oscillations over 600 s. To determine whether these oscillations are similarly regulated by STIM1 and/or STIM2 as those induced by antigenic stimuli, we stimulated RBL-1 cells with LTC_4 and compared cells preincubated with G418 (Fig. 3*F*) to cells left untreated (Fig. 3*E*). The analysis of Ca^{2+} oscillations was done in a time-resolved manner and revealed that G418 preincubation did not affect the number of spikes for the first 400 s of stimulation (Fig. 3*G*), but significantly decreased the number of spikes at later times (Fig. 3*H*), suggesting that STIM2 can support long-lasting LTC_4-induced oscillations.

The above experiments demonstrate that in RBL-2H3 and RBL-1 cells STIM2 is an important component of SOCE. A recent study showed that T cells may also use STIM2, as lymphocytes from STIM2-deficient mice exhibit reduced cytokine expression after phorbol 12-myristate 13-acetate/ionomycin treatment compared to wild-type cells (Oh-Hora *et al.* 2008). The STIM2-deficient T cells failed to sustain a stable nuclear translocation of NFAT; however, these cells did not seem to have reduced SOCE in response to TCR stimulation. We considered the possibility that this puzzling discrepancy may have resulted from differences in experimental conditions used to assess NFAT translocation and Ca^{2+} entry. To test the idea that STIM2 is involved in the receptor-mediated activation of lymphocytes, we stimulated human lymphocytes with anti-CD3 antibody after preincubation with or without G418. The application of 10 μg ml^{-1} anti-CD3 revealed no significant difference between the two conditions (Fig. S7*A*). However, at 2 μg ml^{-1} anti-CD3 antibody, Ca^{2+} influx was significantly suppressed by G418 (Fig. S7*B*), while remaining ineffective in untreated controls (Fig. S7*C*). These results indicate that STIM2 plays a crucial role during submaximal receptor stimulation in human lymphocytes, but in contrast to RBL-2H3 cells, high agonist concentrations do not seem to have a significant STIM2-dependent component of SOCE.

The above experiments demonstrate that STIM2 contributes to SOCE in immunocytes such as mast cells and T cells, in agreement with observations made in dendritic cells (Bandyopadhyay *et al.* 2011) and B cells (Matsumoto *et al.* 2011). In HEK293 cells, however, conflicting results have been published. A recent study by Bird and colleagues has suggested that although STIM2 is endogenously expressed in HEK293 cells, STIM2 itself is not capable of opening CRAC channels in this particular cell type (Bird *et al.* 2009). They reported that Ca^{2+} oscillations induced by low MeCh concentrations cause minimal depletion of ER Ca^{2+} as previously reported (Wedel *et al.* 2007), yet the main driver of SOCE during these oscillations appeared to be STIM1 and not STIM2. This surprising result prompted us to re-investigate the issue by closely reproducing the experimental conditions employed by Bird and colleagues. We confirmed that applying low concentrations (5 μM) of the PLCβ-linked agonist MeCh results in repetitive cytoplasmatic Ca^{2+} spikes in HEK293 cells (Fig. 4*A*); however, these were significantly reduced when preincubating cells with the STIM2 inhibitor G418 (Fig. 4*A*). Similar experiments where performed in Ca^{2+}-free medium and demonstrated that G418 did not affect Ca^{2+} oscillations in the absence of extracellular Ca^{2+} (Fig. 4*B*). To corroborate these observations, we also performed knockdown experiments of STIM1 and STIM2 (Fig. S6), which both substantially reduced the frequency of Ca^{2+} oscillations in HEK293 cells (Fig. 4*C*). However, neither STIM1 nor STIM2 knockdown alone reduced the frequency of the Ca^{2+} oscillations to levels obtained in Ca^{2+}-free medium. These results suggest that MeCh-mediated oscillations in HEK293 cells are regulated by both STIM1 and STIM2, rather than exclusively through STIM1 as previously suggested.

Discussion

In summary, our results provide insight into the relative roles of native STIM1 and STIM2 in regulating SOCE evoked by receptor agonists in some of the most widely studied model systems of mast cells (RBL-1 and RBL-2H3), HEK293 cells and Jurkat T cells. STIM1 and STIM2 are coexpressed in most cell types (Williams *et al.* 2001; Feske, 2007; Oh-Hora *et al.* 2008) and the present study confirms that both molecules can serve to communicate the filling state of the stores to CRAC channel activation, consistent with the findings obtained in heterologous expression systems (Liou *et al.* 2007; Parvez *et al.* 2008). Thus, our results are largely in line with previous reports showing that STIM2 can initiate SOCE (Oh-Hora *et al.* 2008; Bandyopadhyay *et al.* 2011).

Given the lower affinity of STIM2 for luminal ER Ca^{2+}, it is faster translocation into puncta, and its ability to engage in activation of SOCE, it was hypothesized that STIM2 might have a role in mediating Ca^{2+} entry at submaximal receptor stimulation that results in only moderate store depletion. Surprisingly, however, Bird *et al.* (2009) reported that STIM2 does not appear to contribute to SOCE in HEK293 cells and is exclusively regulated by STIM1 even at low-level agonist stimulation and moderate store depletion. A more recent study in RBL-1 cells (Kar *et al.* 2012) essentially confirmed the lack of impact of STIM2 in shaping Ca^{2+} oscillations over a period of 600 s evoked by low concentrations of LTC_4 through G protein-coupled receptor signalling, although it did find a role for STIM2 in low-level stimulation of IgE receptors.

Some of the results presented here are in agreement with previous work, while others are at variance. Some of the discrepancies may relate to the experimental approaches employed. Both of the above studies used siRNA knockdown of STIM proteins at different levels of efficacy over several days to probe STIM function and this could have significant ramifications for interpreting the results. STIM2 is active at rest and regulates the levels of both cytosolic and luminal ER Ca^{2+} levels. Its efficient knockdown over days can lower ER Ca^{2+} levels and thereby reduce the threshold for STIM1-mediated SOCE. This is what we observed in RBL-2H3 cells, where we achieved 87% reduction in STIM2 levels and STIM1 was able to compensate for its loss (see Fig. 2). Bird *et al.* (2009) achieved a similarly strong reduction of STIM2 of 80% in HEK293 cells and observed no effect of STIM2 on MeCh-mediated oscillations, whereas our inhibition of STIM2 expression was ~60% and we did see inhibition of MeCh-induced oscillations. Given the strong inhibition of STIM2 expression obtained by Bird *et al.* it is possible that STIM1 would be able to compensate for the loss of STIM2 and mask the effect of STIM2 reduction. A slightly lower reduction of STIM2 expression of ~60% as achieved in our experiments might be able to maintain sufficient levels of ER Ca^{2+} to prevent STIM1 compensation yet have enough impact to impede SOCE to cause a slight reduction in Ca^{2+} oscillations in HEK293 cells.

Interestingly, Kar *et al.* (2012) achieved a moderate level of STIM2 expression reduction (60%) in RBL-1 cells, which indeed was accompanied by a reduction in antigen-induced oscillations, but did not result in a significant change in GPCR-mediated oscillations up to 600 s. This may not be surprising, as even strong acute suppression of STIM2 using G418 will reveal an effect only at late times of oscillatory activity after 400–1200 s. It thus appears that it is very difficult to assess STIM2 function properly through siRNA knockdown independently of STIM1, given that STIM1's function will be affected by STIM2's ability to regulate ER Ca^{2+} levels at rest. For this reason, G418 offers a useful pharmacological approach to acutely suppress STIM2.

In the present study, using HEK293, RBL and T cells we used stimuli that generate signals through protein G coupled receptors as well as tyrosine kinase pathways that cause PLCβ-mediated and PLCγ-mediated IP_3 production. For each of these stimulation protocols we found that STIM1 and STIM2 participate in mediating SOCE to different extent and dependent on the degree of store depletion. In RBL and T cells, STIM2 is the predominant signalling molecule at low levels of agonist stimulation and STIM1 is progressively recruited with higher agonist concentrations. Although its relative contribution decreases with increasing agonist concentrations, STIM2 remains effective in RBL cells, whereas in T cells, STIM2 is most prominent at low agonist

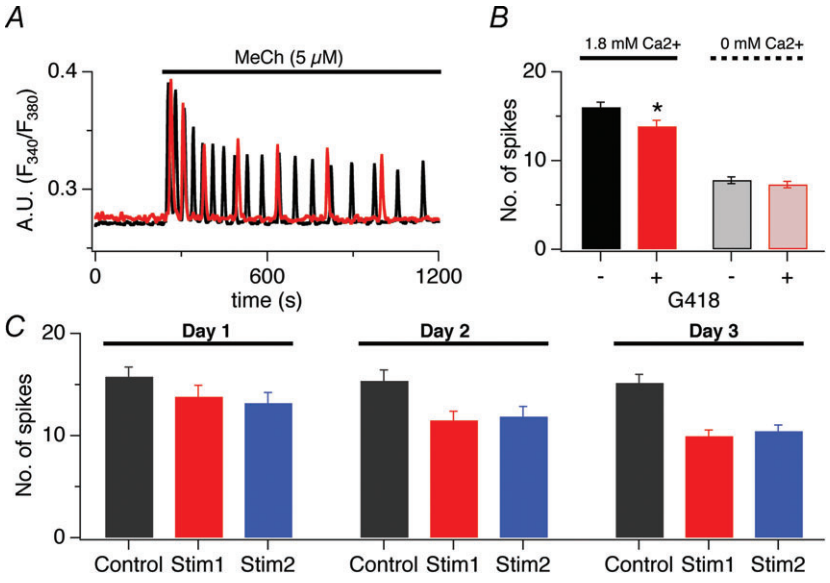

Figure 4. Effects of G418 and STIM knockdown on MeCh-induced Ca^{2+} oscillations
A, intracellular Ca^{2+} changes (F_{340}/F_{380}) after 5 μM MeCh stimulation in two single representative HEK293 cells in the absence or preincubated for 1 h with 500 μg ml^{-1} G418. *B*, average rate of spikes during 1200 s ($P < 0.001$) after MeCh stimulation (5 μM) for cells in the absence or preincubated for 1 h with 500 μg ml^{-1} G418 and performed in the absence or presence of external Ca^{2+}. Error bars indicate S.E.M. *C*, similar experiments were performed when cells were transfected with control siRNA or siRNA directed against STIM1 or STIM2 and analysed on days 1, 2 and 3 post-transfection. kd, knockdown; MeCh, metacholine; STIM, stromal cell-interaction molecule.

stimulation and completely replaced by STIM1 at higher concentrations. In HEK293 cells, STIM1 and STIM2 both contribute to MeCh-induced Ca^{2+} oscillations with similar relative contributions.

Our results indicate that while both endogenous STIM1 or STIM2 are able to open all available endogenous Orai channels (Fig. 1*C*), as has been proposed previously (Bird *et al.* 2009), they do so through progressively activating CRAC channels as a function of store depletion (Fig. 1*A*). Therefore, it appears that these molecules are not simply redundant Ca^{2+} sensors, but serve specific physiological functions. When strongly stimulating IgE receptors in RBL-2H3 we find that about one-third of the overall Ca^{2+} signal generated is mediated by STIM2, whereas maximal stimulation of T cells through TCR reveals no significant contribution of STIM2. This latter observation is in agreement with results obtained in mouse T cells derived from STIM2 knockout animals where strong TCR stimulation produced identical Ca^{2+} responses in wild-type and STIM2 knockout cells (Oh-Hora *et al.* 2008). However, our experiments probing Ca^{2+} entry during low levels of receptor stimulation demonstrate that SOCE is primarily activated through STIM2, both in mast cells and T cells. This would indicate that the experimental protocol employed to demonstrate STIM2 function through NFAT translocation following phorbol 12-myristate 13-acetate/ionomycin stimulation (Oh-Hora *et al.* 2008) may have established conditions that caused mild store depletion.

The present study also highlights that Ca^{2+} signals measured in intact cells may not necessarily yield the same quantitative results as patch clamp recordings. Thus, in patch clamp experiments and controlled store depletion protocols, it is possible to establish conditions where I_{CRAC} is almost exclusively controlled by STIM2, whereas Ca^{2+} signals in intact cells show more of a mixed reaction. The reason for this discrepancy may be due to several factors. An important consideration is that Ca^{2+} entry through CRAC channels is subject to Ca^{2+}-dependent inactivation (Hoth & Penner, 1993; Zweifach & Lewis, 1995), so that Ca^{2+} signals in intact cells are to a large degree self-limited. It is presently unknown whether STIM1- and STIM2-coupled CRAC channel complexes exhibit different Ca^{2+}-dependent regulation. However, STIM2 is specifically regulated by calmodulin (Parvez *et al.* 2008), making that a very real possibility. Additionally, in a model respecting the three-dimensional architecture of a cell the possible formation of a Ca^{2+} gradient could explain how a given stimulus generates the coexistence of ER Ca^{2+} stores with differing filling states, allowing activation of STIM1 close to the plasma membrane and STIM2 closer to the centre of the cell.

In addition, one has to consider that STIM1 and STIM2 molecules aggregate and co-assemble into clusters upon store depletion (Darbellay *et al.* 2010). The signalling mechanism therefore may include both molecules, even if the initial response might be mediated by STIM2 due to its lower Ca^{2+} affinity (Zheng *et al.* 2008). This could also explain why STIM1 knockdown affects Ca^{2+} entry and oscillations at low agonist concentrations. A further caveat in assessing STIM2 function arises in knockdown or knockout studies, as long-term suppression of STIM2 itself can lower the Ca^{2+} contents of stores (Fig. 2*G*–*I*; Brandman *et al.* 2007), so that mild store depletion in these cells may affect STIM1 function, causing earlier activation and leading to functional compensation for the loss STIM2. Another complicating factor that needs to be considered is the growing evidence for Ca^{2+} store heterogeneity, pointing to a specialized store that is functionally coupled to SOCE (Parekh *et al.* 1997; Peinelt *et al.* 2009). In RBL cells, it was found that a large fraction of ER Ca^{2+} could be released by low submicromolar concentrations of IP_3 without triggering CRAC channel activation; increasing IP_3 above $\sim 3\,\mu M$ then activates I_{CRAC} without significant release signals, presumably from a subcompartment that specifically regulates SOCE (Parekh *et al.* 1997).

In summary, we believe that the present study highlights the importance of both STIM1 and STIM2 in regulating SOCE. These sensors may enable cells to sense the degree of receptor stimulation and endow the STIM/CRAC channel complex to be differentially regulated by feedback mechanisms, thereby shaping oscillatory changes in Ca^{2+} as well as the refilling of stores.

References

Bandyopadhyay BC, Pingle SC & Ahern GP (2011). Store-operated Ca^{2+} signaling in dendritic cells occurs independently of STIM1. *J Leukoc Biol* **89**, 57–62.

Bird GS, Hwang SY, Smyth JT, Fukushima M, Boyles RR & Putney JW (2009). STIM1 is a calcium sensor specialized for digital signaling. *Curr Biol* **19**, 1724–1729.

Brandman O, Liou J, Park WS & Meyer T (2007). STIM2 is a feedback regulator that stabilizes basal cytosolic and endoplasmic reticulum Ca^{2+} levels. *Cell* **131**, 1327–1339.

Broad LM, Armstrong DL & Putney JW (1999). Role of the inositol 1,4,5-trisphosphate receptor in Ca^{2+} feedback inhibition of calcium release-activated calcium current (ICRAC). *J Biol Chem* **274**, 32881–32888.

Di Capite J, Ng SW & Parekh AB (2009). Decoding of cytoplasmic Ca^{2+} oscillations through the spatial signature drives gene expression. *Curr Biol* **19**, 853–858.

Darbellay B, Arnaudeau S, Ceroni D, Bader CR, Konig S & Bernheim L (2010). Human muscle economy myoblast differentiation and excitation-contraction coupling use the same molecular partners, STIM1 and STIM2. *J Biol Chem* **285**, 22437–22447.

Dormer RL, Capurro DE, Morris R & Webb R (1993). Demonstration of two isoforms of the SERCA-2b type Ca^{2+},Mg^{2+}-ATPase in pancreatic endoplasmic reticulum. *Biochim Biophys Acta* **1152**, 225–230.

Dziadek MA & Johnstone LS (2007). Biochemical properties and cellular localisation of STIM proteins. *Cell Calcium* **42**, 123–132.

Ehring GR, Kerschbaum HH, Fanger CM, Eder C, Rauer H & Cahalan MD (2000). Vanadate induces calcium signaling, Ca^{2+} release-activated Ca^{2+} channel activation, and gene expression in T lymphocytes and RBL-2H3 mast cells via thiol oxidation. *J Immunol* **164**, 679–687.

Feske S (2007). Calcium signalling in lymphocyte activation and disease. *Nat Rev Immunol* **7**, 690–702.

Feske S, Gwack Y, Prakriya M, Srikanth S, Puppel S-H, Tanasa B, Hogan PG, Lewis RS, Daly M & Rao A (2006). A mutation in Orai1 causes immune deficiency by abrogating CRAC channel function. *Nature* **441**, 179–185.

Gwack Y, Srikanth S, Feske S, Cruz-Guilloty F, Oh-hora M, Neems DS, Hogan PG & Rao A (2007). Biochemical and functional characterization of Orai proteins. *J Biol Chem* **282**, 16232–16243.

Hoth M & Penner R (1992). Depletion of intracellular calcium stores activates a calcium current in mast cells. *Nature* **355**, 353–356.

Hoth M & Penner R (1993). Calcium release-activated calcium current in rat mast cells. *J Physiol* **465**, 359–386.

Kar P, Bakowski D, Di Capite J, Nelson C & Parekh AB (2012). Different agonists recruit different stromal interaction molecule proteins to support cytoplasmic Ca^{2+} oscillations and gene expression. *Proc Natl Acad Sci U S A* **109**, 6969–6974.

Lewis RS (2007). The molecular choreography of a store-operated calcium channel. *Nature* **446**, 284–287.

Liou J, Fivaz M, Inoue T & Meyer T (2007). Live-cell imaging reveals sequential oligomerization and local plasma membrane targeting of stromal interaction molecule 1 after Ca^{2+} store depletion. *Proc Natl Acad Sci U S A* **104**, 9301–9306.

Lioudyno MI, Kozak JA, Penna A, Safrina O, Zhang SL, Sen D, Roos J, Stauderman KA & Cahalan MD (2008). Orai1 and STIM1 move to the immunological synapse and are up-regulated during T cell activation. *Proc Natl Acad Sci U S A* **105**, 2011–2016.

Lis A, Peinelt C, Beck A, Parvez S, Monteilh-Zoller M, Fleig A & Penner R (2007). CRACM1, CRACM2, and CRACM3 are store-operated Ca^{2+} channels with distinct functional properties. *Curr Biol* **17**, 794–800.

Luik RM, Wu MM, Buchanan J & Lewis RS (2006). The elementary unit of store-operated Ca^{2+} entry: local activation of CRAC channels by STIM1 at ER-plasma membrane junctions. *J Cell Biol* **174**, 815–825.

Matsumoto M, Fujii Y, Baba A, Hikida M, Kurosaki T & Baba Y (2011). The calcium sensors STIM1 and STIM2 control B cell regulatory function through interleukin-10 production. *Immunity* **34**, 703–714.

Mercer JC, Dehaven WI, Smyth JT, Wedel B, Boyles RR, Bird GS & Putney JW (2006). Large store-operated calcium selective currents due to co-expression of Orai1 or Orai2 with the intracellular calcium sensor, Stim1. *J Biol Chem* **281**, 24979–24990.

Oh-Hora M, Yamashita M, Hogan PG, Sharma S, Lamperti E, Chung W, Prakriya M, Feske S & Rao A (2008). Dual functions for the endoplasmic reticulum calcium sensors STIM1 and STIM2 in T cell activation and tolerance. *Nat Immunol* **9**, 432–443.

Parekh AB & Putney JW (2005). Store-operated calcium channels. *Physiol Rev* **85**, 757–810.

Parekh AB, Fleig A & Penner R (1997). The store-operated calcium current I(CRAC): nonlinear activation by InsP3 and dissociation from calcium release. *Cell* **89**, 973–980.

Parvez S, Beck A, Peinelt C, Soboloff J, Lis A, Monteilh-Zoller M, Gill DL, Fleig A & Penner R (2008). STIM2 protein mediates distinct store-dependent and store-independent modes of CRAC channel activation. *FASEB J* **22**, 752–761.

Peinelt C, Vig M, Koomoa DL, Beck A, Nadler MJS, Koblan-Huberson M, Lis A, Fleig A, Penner R & Kinet J-P (2006). Amplification of CRAC current by STIM1 and CRACM1 (Orai1). *Nat Cell Biol* **8**, 771–773.

Peinelt C, Beck A, Monteilh-Zoller MK, Penner R & Fleig A (2009). IP(3) receptor subtype-dependent activation of store-operated calcium entry through I(CRAC). *Cell Calcium* **45**, 326–330.

Prakriya M, Feske S, Gwack Y, Srikanth S, Rao A & Hogan PG (2006). Orai1 is an essential pore subunit of the CRAC channel. *Nature* **443**, 230–233.

Putney JW (2007). New molecular players in capacitative Ca^{2+} entry. *J Cell Sci* **120**, 1959–1965.

Renner C, Jung W, Sahin U, Van Lier R & Pfreundschuh M (1995). The role of lymphocyte subsets and adhesion molecules in T cell-dependent cytotoxicity mediated by CD3 and CD28 bispecific monoclonal antibodies. *Eur J Immunol* **25**, 2027–2033.

Roos J, DiGregorio PJ, Yeromin AV, Ohlsen K, Lioudyno M, Zhang S, Safrina O, Kozak JA, Wagner SL, Cahalan MD, Velicelebi G & Stauderman KA (2005). STIM1, an essential and conserved component of store-operated Ca^{2+} channel function. *J Cell Biol* **169**, 435–445.

Smyth JT, Dehaven WI, Bird GS & Putney JW (2008). Ca^{2+}-store-dependent and -independent reversal of Stim1 localization and function. *J Cell Sci* **121**, 762–772.

Soboloff J, Spassova MA, Hewavitharana T, He LP, Xu W, Johnstone LS, Dziadek MA & Gill DL (2006). STIM2 is an inhibitor of STIM1-mediated store-operated Ca^{2+} entry. *Curr Biol* **16**, 1465–1470.

Stathopulos PB, Li GY, Plevin MJ, Ames JB & Ikura M (2006). Stored Ca^{2+} depletion-induced oligomerization of stromal interaction molecule 1 (STIM1) via the EF-SAM region: an initiation mechanism for capacitive Ca^{2+} entry. *J Biol Chem* **281**, 35855–35862.

Thastrup O, Cullen PJ, Drobak BK, Hanley MR & Dawson AP (1990). Thapsigargin, a tumor promoter, discharges intracellular Ca^{2+} stores by specific inhibition of the endoplasmic reticulum Ca^{2+}-ATPase. *Proc Natl Acad Sci U S A* **87**, 2466–2470.

Turner H, Fleig A, Stokes A, Kinet J-P & Penner R (2003). Discrimination of intracellular calcium store subcompartments using TRPV1 (transient receptor potential channel, vanilloid subfamily member 1) release channel activity. *Biochem J* **371**, 341–350.

Vig M, Beck A, Billingsley JM, Lis A, Parvez S, Peinelt C, Koomoa DL, Soboloff J, Gill DL, Fleig A, Kinet J-P & Penner R (2006*a*). CRACM1 multimers form the ion-selective pore of the CRAC channel. *Curr Biol* **16**, 2073–2079.

Vig M, Peinelt C, Beck A, Koomoa DL, Rabah D, Koblan-Huberson M, Kraft S, Turner H, Fleig A, Penner R & Kinet JP (2006*b*). CRACM1 is a plasma membrane protein essential for store-operated Ca^{2+} entry. *Science* **312**, 1220–1223.

Wedel B, Boyles RR, Putney JW & Bird GS (2007). Role of the store-operated calcium entry proteins Stim1 and Orai1 in muscarinic cholinergic receptor-stimulated calcium oscillations in human embryonic kidney cells. *J Physiol* **579**, 679–689.

Williams RT, Manji SS, Parker NJ, Hancock MS, Van Stekelenburg L, Eid JP, Senior PV, Kazenwadel JS, Shandala T, Saint R, Smith PJ & Dziadek MA (2001). Identification and characterization of the STIM (stromal interaction molecule) gene family: coding for a novel class of transmembrane proteins. *Biochem J* **357**, 673–685.

Wu MM, Buchanan J, Luik RM & Lewis RS (2006). Ca^{2+} store depletion causes STIM1 to accumulate in ER regions closely associated with the plasma membrane. *J Cell Biol* **174**, 803–813.

Wu MM, Luik RM & Lewis RS (2007). Some assembly required: constructing the elementary units of store-operated Ca^{2+} entry. *Cell Calcium* **42**, 163–172.

Xu P, Lu J, Li Z, Yu X, Chen L & Xu T (2006). Aggregation of STIM1 underneath the plasma membrane induces clustering of Orai1. *Biochem Biophys Res Commun* **350**, 969–976.

Yeromin AV, Zhang SL, Jiang W, Yu Y, Safrina O & Cahalan MD (2006). Molecular identification of the CRAC channel by altered ion selectivity in a mutant of Orai. *Nature* **443**, 226–229.

Yuan JP, Zeng W, Dorwart MR, Choi YJ, Worley PF & Muallem S (2009). SOAR and the polybasic STIM1 domains gate and regulate Orai channels. *Nat Cell Biol* **11**, 337–343.

Zhang SL, Yu Y, Roos J, Kozak JA, Deerinck TJ, Ellisman MH, Stauderman KA & Cahalan MD (2005). STIM1 is a Ca^{2+} sensor that activates CRAC channels and migrates from the Ca^{2+} store to the plasma membrane. *Nature* **437**, 902–905.

Zheng L, Stathopulos PB, Li GY & Ikura M (2008). Biophysical characterization of the EF-hand and SAM domain containing Ca^{2+} sensory region of STIM1 and STIM2. *Biochem Biophys Res Commun* **369**, 240–246.

Zweifach A & Lewis RS (1995). Rapid inactivation of depletion-activated calcium current (ICRAC) due to local calcium feedback. *J Gen Physiol* **105**, 209–226.

Author contributions

Conception and design, data interpretation and manuscript writing (R.P.); conception and design, collection and assembly of data, data analysis and interpretation, manuscript writing (M.T. and A.L.). All authors approved the final version of the manuscript.

Acknowledgements

We thank S. Johne, L. Tsue and C. Wakano for excellent technical support. We also thank Drs A. Fleig and J. Starkus for critically reading the manuscript. The use of human material was approved by the Queen's Medical Center Research and Institutional Review Committee (RIRC). The authors have no conflict of interest. This work was supported by DFG grant Li 1750/1–1 (A.L.), QERF (M.T.), NIH/NAID R01AI050200 and NIH/NIGMS R01GM080555 (R.P.).